

IBM Research Report

Strain Relaxation and Threading Dislocation Density in Helium-Implanted and Annealed $\text{Si}_{1-x}\text{Ge}_x/\text{Si}$ (100) Heterostructures

J. Cai¹, P. M. Mooney¹, S. H. Christensen¹, H. Chen², J. O. Chu¹, J. A. Ott¹

¹IBM Research Division
Thomas J. Watson Research Center
P.O. Box 218
Yorktown Heights, NY 10598

²IBM Microelectronics Division
Hopewell Junction, NY



Research Division

Almaden - Austin - Beijing - Haifa - India - T. J. Watson - Tokyo - Zurich

Strain relaxation and threading dislocation density in helium-implanted and annealed $\text{Si}_{1-x}\text{Ge}_x/\text{Si}$ (100) heterostructures

J. Cai^a, P.M. Mooney^a, S.H. Christiansen^{a*}, H. Chen^b, J.O. Chu^a, and J.A. Ott^a

IBM Research and Development Center,

^aT. J. Watson Research Center, Yorktown Heights, NY, USA

^bMicroelectronics Division, Hopewell Junction, NY, USA

Abstract

Strain relaxation and threading dislocation densities in $\text{Si}_{1-x}\text{Ge}_x$ ($0.15 < x < 0.30$) produced by He implantation and annealing have been investigated using x-ray diffraction and transmission electron microscopy. The degree of strain relaxation is very sensitive to the SiGe layer thickness; only small differences in strain relaxation are obtained when the helium dose and energy are varied over a relatively wide range. In contrast, the threading dislocation density is strongly influenced by the implantation dose and depth. A composite parameter, the He dose in the SiGe layer ($\text{He}(\text{SiGe})$), calculated from He profiles simulated using the program Stopping and Range of Ions in Matter (SRIM2000), correlates well with the threading dislocation density. We have found that to achieve a low threading dislocation density, $< 5 \times 10^7 \text{ cm}^{-2}$, $\text{He}(\text{SiGe})$ must be less than $1 \times 10^{15} \text{ cm}^{-2}$.

*Present address: MPI-Mikrostrukturphysik, Halle, Germany.

I. INTRODUCTION

Strain-relaxed $\text{Si}_{1-x}\text{Ge}_x$ alloys are used as virtual substrates for strained Si devices in which the electron and hole mobility is enhanced compared to devices fabricated in unstrained Si.^{1,2} When SiGe layers are grown epitaxially on Si(001) substrates, the strain is relaxed by plastic deformation, i.e., misfit dislocations are formed when the strain in the layers exceeds the critical value.³⁻⁵ Ideally, misfit dislocations would be nucleated and would glide to the edge of the sample, leaving a network of misfit dislocations at interfaces. However, in practice a large number of dislocations are nucleated. After gliding a short distance they become immobilized, resulting in SiGe layers with a very high density of threading dislocations.

In order to achieve useful materials for device applications, we need to find methods to produce SiGe layers with the following properties: a high degree of strain relaxation, a low threading dislocation density, and a flat surface. Traditionally, device-quality relaxed SiGe buffer layers have been achieved by growth of a very thick compositionally graded $\text{Si}_{1-x}\text{Ge}_x$ layer on Si. Nearly completely relaxed $\text{Si}_{1-x}\text{Ge}_x$ ($0.1 < x < 1$) with threading dislocation densities of $1 \times 10^5 - 5 \times 10^7 \text{ cm}^{-2}$ have been demonstrated.^{6,7} Despite the low threading dislocation density, there are problems when using these layers for CMOS applications. First, these layers have rough surfaces, typically a root mean square (RMS) surface roughness of $\sim 6 \text{ nm}$ when $x=0.3$. Therefore an extra process to planarize the surface, for example, chemical-mechanical polishing, has to be applied before growing device structures, thus increasing the cost. In addition, the thermal conductivity of SiGe is lower than that of pure Si. Therefore using a thick graded buffer layers result in poor heat conductivity, which may be troublesome for applications in ultra large scale integrated circuits.

It is well known that ion-implantation into SiGe enhances strain relaxation. For example, regions of SiGe layers implanted with B or As relax more upon annealing than do regions that were not implanted.⁸ In another example, misfit dislocations were found to nucleate preferentially during growth of SiGe layers in regions where the Si substrate had been implanted with Ge.⁹ More recently, ion-implantation of He and H₂ were proposed as an alternative way to obtain high quality SiGe buffer layers. The core idea is to implant H₂ or He into pseudomorphic SiGe layers to introduce a damage layer below the SiGe/Si interface.^{10,11} During subsequent annealing, dislocations nucleated in the damage layer glide or climb to the SiGe/Si interface and relieve the mismatch strain. It was reported that thin SiGe layers having a high degree of relaxation as well as relatively low threading dislocation density can be achieved by helium implantation and subsequent annealing at temperatures of 750-850 °C.¹⁰⁻¹²

We have studied strain relaxation and the defect density of SiGe buffer layers produced by He implantation and annealing. An initial transmission electron microscopy (TEM) study of 100nm-thick Si_{1-x}Ge_x (x=0.15) layers, showed that the implant damage, and also the relaxation mechanism, varies with implantation conditions, even though the degree of strain relaxation was found to be similar.¹² Here we present results of a larger study of the effects of experimental parameters such as SiGe layer thickness and alloy composition and implantation conditions on the properties of SiGe virtual substrates. We find that the degree of strain relaxation is strongly dependent on the SiGe layer thickness and only weakly dependent on the He dose and depth. In contrast, we also find that the threading dislocation density is very sensitive to the He implantations conditions. There is a strong correlation between the amount of He implanted into the SiGe layer, He(SiGe), and the threading dislocation density.

II. Experimental Methods

Pseudomorphic $\text{Si}_{1-x}\text{Ge}_x$ layers ($0.15 < x < 0.30$) were grown on Si (100) by ultra high vacuum chemical vapor deposition (UHVCVD) on 200 mm Si(001) substrates and by rapid thermal chemical vapor deposition (RTCVD) on both 200 and 300 mm Si(001) substrates. He^+ ions were then implanted into the wafers at room temperature. The implantation energy was chosen so that the projected range (R_p) of He atoms obtained using the simulation software SRIM2000 is below the SiGe/Si interface. Fig. 1 shows a simulated helium profile for a 196 nm thick $\text{Si}_{0.7}\text{Ge}_{0.3}$ layer on a Si substrate implanted with 38 keV He^+ . In order to compare SiGe layers of different thickness, we define a parameter D , the implantation depth below the SiGe/Si interface, as R_p minus t , the SiGe layer thickness. After implantation, wafers were annealed in a He or N_2 ambient, at a temperature of 800 or 850°C for 12 minutes or longer.

High-resolution x-ray diffraction (XRD) was used to measure layer thickness and Ge composition of the as-grown pseudomorphic SiGe layers at the wafer center, and also the degree of strain relaxation of the SiGe layer in each sample after annealing. X-ray measurements were performed using a Philips XPert Pro diffraction system equipped with a hybrid incident beam monochromator consisting of a mirror and a four-bounce Ge crystal that gives a 1mm x 10mm incident Cu- K_α beam ($\lambda = 1.542 \text{ \AA}$) with a divergence of 0.007° . For the relaxed layers, both symmetric (004) and asymmetric (224) reflections were measured by XRD. The degree of strain relaxation was calculated by

$$\% \text{ strain relaxation} = \frac{a_l - a_s}{a_l^R - a_s} \times 100\% ,$$

where a_l and a_s are the in-plane lattice constants of the $\text{Si}_{1-x}\text{Ge}_x$ layer and the Si substrate, respectively, and a_l^R is the lattice constant of fully relaxed $\text{Si}_{1-x}\text{Ge}_x$. The uncertainty in the Ge mole fraction is ± 0.01 and in the strain relaxation is $\pm 3\%$. Surface features were measured by atomic force microscopy (AFM) using a Digital Instruments Dimension 5000 Nanoscope. Plan-view transmission electron microscopy (PVTEM) was used to determine the threading dislocation density. TEM samples were prepared by standard mechanical thinning and ion milling techniques. The observations were performed in a CM12 microscope operating at 120 kV. Threading dislocations were counted in an area of $360 \mu\text{m}^2$ for samples with a density of 10^7 cm^{-2} , with a typical uncertainty of $\pm 30\%$.

III. RESULTS AND DISCUSSION

The relationship between strain relaxation and SiGe layer thickness is shown in Fig. 2. Fig. 2(a) compares $\text{Si}_{1-x}\text{Ge}_x$ samples with $x=0.15$ and $x=0.20$ grown by UHVCVD. The He^+ dose was the same, $1 \times 10^{16} \text{ cm}^{-2}$, for all these samples and the implantation energy was varied to give a depth, D , of 140-200 nm. For both alloy compositions, the degree of strain relaxation increases with the layer thickness, saturating at a value of $\sim 85\%$. A high degree of strain relaxation ($>70\%$) is achieved only when the SiGe thickness is >200 nm. The scatter in the data is due to the variation of the SiGe layer thickness across the wafer. The degree of strain relaxation was found to be the same for annealing at both 800 and 850 °C and for times of 12-60 minutes. Comparing with pieces of the wafer that were not implanted but were annealed under the same conditions, He implantation before annealing greatly enhances the strain relaxation, even for the thickest SiGe layers. Fig. 2(b) compares $\text{Si}_{0.8}\text{Ge}_{0.2}$ samples grown by UHVCVD and RTCVD. Again the He^+ dose and implant depth, D , were similar for all the samples. Clearly the degree of strain relaxation is the same for samples grown by both methods.

Fig. 3(a) compares Si_{0.7}Ge_{0.3} layers with and without He implants after annealing. The He dose was $1 \times 10^{16} \text{ cm}^{-2}$ and the depth, D , was 150-200 nm. Again we see that the degree of strain relaxation increases with the layer thickness and is enhanced by the He implant. Fig. 3(b) shows the effects of varying the He implantation dose and depth on the strain relaxation of Si_{0.7}Ge_{0.3}. The strain relaxation of thick films ($t=196 \text{ nm}$) is about 85%, and it is insensitive to the implantation depth and dose. For thinner films, increasing the He dose affects the degree of strain relaxation. This is shown for 143 nm-thick films with very deep implants and for 92 nm-thick films with very shallow implants. However, the total degree of relaxation of ion-implanted samples is much more sensitive to the SiGe layer thickness than to the He⁺ implantation conditions.

The surfaces of ion implanted and annealed buffer (IAB) layers are relatively smooth. The root mean square (RMS) surface roughness is in the range of 0.2-0.6 nm. However, we have also observed two types of surfaces on the IAB layers. Both types of surfaces show straight-line cross hatch features running along perpendicular [110] axes, which correspond to the misfit dislocations that relieve the strain.¹³ One type of surface, shown in Fig. 4(a), exhibits a pattern of long, straight lines indicating the presence of long misfit dislocations, whereas the other type, shown in Fig. 4(b), exhibits a patchy surface of short straight lines indicating the presence of much shorter misfit dislocations in these samples. Although the RMS roughness of these two type surfaces is quite similar and the degree of strain relaxation in both types of samples is comparable, the threading dislocation densities in these SiGe layers are very different. Consistent with the observation of short misfit dislocations, PVTEM images show that samples with patchy surfaces always have a very high density of threading dislocations ($>10^9 \text{ cm}^{-2}$).

Fig. 5 compares misfit dislocations in two $\text{Si}_{0.7}\text{Ge}_{0.3}$ samples with similar strain relaxation ($\sim 75\%$) but very different surface features. The sample with deep helium implantation has an array of long, straight misfit dislocations at the SiGe/Si interface, shown in Fig. 5(a), and it has a surface feature similar to Fig. 4(a). This SiGe layer has a relatively low threading dislocation, $4.4 \times 10^7 \text{ cm}^{-2}$. In contrast, Fig. 5(b) shows a high density of helium bubbles and an irregular array of misfit dislocations in a sample with shallow helium implantation. This sample has a very high density of threading dislocations, $2.7 \times 10^{10} \text{ cm}^{-2}$, and its surface looks like that in Fig. 4(b).

Comparing samples with a variety of implant doses and implant depths, we have found that the amount of He implanted into the SiGe layer correlates strongly with the threading dislocation density. We introduce a parameter, the amount of He in the SiGe layer, as a measure of the damage in the SiGe layer caused by the He implantation. $\text{He}(\text{SiGe})$ is defined as the integral of the He profile over the SiGe layer thickness, i.e., $\int_0^t [\text{He}] dx$. For example, the He dose in the SiGe layer shown in Fig. 1 is 12% of the total implanted He dose.

Fig. 6 shows the threading dislocation density plotted against $\text{He}(\text{SiGe})$ for both UHVCVD- and RTCVD-grown $\text{Si}_{1-x}\text{Ge}_x$ layers. The threading dislocation density increases strongly with $\text{He}(\text{SiGe})$. When the amount of He increases by one order of magnitude, from $3 \times 10^{14} \text{ cm}^{-2}$ to $4 \times 10^{15} \text{ cm}^{-2}$, the threading dislocation density increases by three orders of magnitude. Fig. 6(a) shows the plot for $\text{Si}_{0.8}\text{Ge}_{0.2}$ layers; whenever $\text{He}(\text{SiGe})$ is greater than $2 \times 10^{15} \text{ cm}^{-2}$, the threading dislocation density is higher than 10^9 cm^{-2} , and samples have patchy surfaces like that shown in Fig. 4(b). In contrast, a low threading dislocation density ($< 5 \times 10^7 \text{ cm}^{-2}$) is obtained when $\text{He}(\text{SiGe})$ is $< 10^{15} \text{ cm}^{-2}$. A similar

behavior is seen for $\text{Si}_{0.7}\text{Ge}_{0.3}$ layers in Fig. 6(b). *Both plots suggest that the lower limit for the threading dislocation density is $\sim 10^7 \text{ cm}^{-2}$.*

Fig. 6 also shows that layers with a high degree of strain relaxation are not always accompanied by high density of threading dislocations. Take for instance Fig. 6(b): The 143 nm $\text{Si}_{0.7}\text{Ge}_{0.3}$ layers have a higher degree of relaxation than the 92 nm layers, but the threading dislocation density in the 143 nm layers is lower. Therefore, by carefully choosing layer thickness and implantation conditions, SiGe layers with both a high degree of strain relaxation and a relatively low density of threading dislocation can be produced by He implantation and annealing.

We now turn to a brief discussion of strain relaxation mechanisms. It is known from earlier work that He implanted below the SiGe/Si interface agglomerates into bubbles and/or platelets during annealing, and dislocation loops are punched out around them.¹¹ These loops glide or climb to the SiGe/Si interface, and misfit dislocations that relieve the mismatch strain in the SiGe layer are formed.^{11,12} Because helium implantation and annealing provides a high density of nucleation sources for dislocations, the strain relaxation in the SiGe layer is enhanced compared to samples with no implant. Provided there are enough dislocation sources, the final degree of strain relaxation depends on the initial elastic strain energy in the film, which in turn only depends on the layer thickness, for layers with a given germanium composition.¹⁴⁻¹⁸ This explains our observation that the degree of relaxation in the thicker SiGe layers depends only on the layer thickness, even though the He implantation conditions are different. However, in the case of thinner layers where there is a lower driving force for strain relaxation, increasing the He dose or reducing the implantation depth slightly increases the degree of strain relaxation, as shown in Fig. 3(b). For a given SiGe layer thickness, reducing the

implant depth and/or increasing the implant dose increases the value of $\text{He}(\text{SiGe})$, and also results in a high threading dislocation density. When $\text{He}(\text{SiGe})$ is relatively high, two mechanisms may cause a high threading dislocation density in SiGe. One possibility is that a large number of dislocation loops are nucleated within SiGe layer during annealing because of the high concentration of helium bubbles there. Since the density of loops is very high, each one will be able to glide for only a short distance, before reaching an area of low strain. Alternatively, the high density of bubbles or other implantation damage in the SiGe layer may impede dislocation glide, forcing additional misfit dislocation nucleation to occur in order to relieve the strain. In either case, the end result will be short misfit dislocations and a very high density of threading dislocations. In contrast, higher-dose deeper implants are better solutions, because they provide increased strain relaxation as well as a relatively low density of threading dislocations. Our observation of a lower limit of $1 \times 10^7 \text{ cm}^{-3}$ for the threading dislocation density suggests that dislocation interactions play an important role in strain relaxation, as has also been shown by numerical simulations¹⁹.

IV. Conclusions

We have demonstrated in this study that highly relaxed $\text{Si}_{1-x}\text{Ge}_x$ layers (>75%) with a RMS surface roughness <0.6 nm, and threading dislocation density less than $5 \times 10^7 \text{ cm}^{-2}$ can be achieved by helium implantation and annealing. The degree of strain relaxation and the defect density in the final SiGe layers are similar for layers grown by UHVCVD and RTCVD. We find that the layer thickness and the amount of helium implanted into SiGe are two key parameters, which greatly influence the degree of strain relaxation and the threading dislocation density, respectively. Our results also suggest that 10^7 cm^{-2} is the lower limit for the threading dislocation density in He-implanted and annealed SiGe buffer layers.

ACKNOWLEDGEMENTS:

We gratefully acknowledge the assistance of D.L. Lacey with XRD measurements, and P.A. Saunders with helium implantations.

REFERENCES:

1. K. Ismail, B. S. Meyerson, and P. J. Wang, *Appl. Phys. Lett.* **58**, 2117 (1991).
2. Y. J. Mii, Y. H. Xie, E. A. Fitzgerald, D. Monrow, F. A. Thiel, B. E. Weir, and L. C. Feldman, *Appl. Phys. Lett.* **59**, 1611 (1991).
3. J. H. Van der Merwe, *J. Appl. Phys.* **34**, 117 (1963).
4. J. H. Van der Merwe, *J. Appl. Phys.* **34**, 123 (1963).
5. E. A. Fitzgerald, *Mater. Sci. Rep.* **7**, 87 (1991).
6. F. K. LeGoues, B. S. Meyerson, J. F. Morar, and P. D. Kirchner, *J. Appl. Phys.* **71**, 4203 (1992).
7. E. A. Fitzgerald, Y. -H. Xie, D. Monroe, P. J. Silverman, J. M. Kuo, A. R. Kortan, F. A. Thiel, and B. E. Weir, *J. Vac. Sci. Technol.* **B10**, 1807 (1992).
8. R. Hull, J.C. Bean, J.M. Bonar, G.S. Higashi, K.T. Short, H. Temkin, and A.E. White, *Appl. Phys. Lett.* **56**, 2445 (1990).
9. J. P. Watson, E.A. Fitzgerald, Y.-H. Xie, P.J. Silverman, A.E. White, and K.T. Short, *Appl. Phys. Lett.* **63**, 764 (1993).
10. S. Mantl, B. Holländer, R. Liedtke, St. Mesters, H. -J. Herzog, H. Kibbel, and T. Hackbarth, *Nucl. Instrum. Methods Phys. Res.* **B147**, 29 (1999).
11. M. Luysberg, D. Kirch, H. Trinkaus, B. Holländer, St. Lenk, S. Mantl, H.-J. Herzog, T. Hackbarth, P. F. P. Fichtner, *J. Appl. Phys.* **92**, 4290 (2002).
12. S. H. Christiansen, P. M. Mooney, J. O. Chu and A. Grill, *Mat. Res. Soc. Symp. Proc.* **686**, 27 (2002).
13. M. A. Lutz, R. M. Feenstra, F. K. LeGoues, P. M. Mooney, and J. O. Chu, *Appl. Phys. Lett.* **66**, 724 (1995).
14. J. H. van der Merwe, *Surf. Sci.* **31**, 198 (1972).

15. J. H. van der Merwe and C. A. B. Ball, in *Epitaxial Growth*, edited by J. W. Matthews (Academic, New York, 1975), Part B, Chap. 6.
16. J. W. Mathews, *J. Vac. Sci. Technol.* **12**, 126 (1975).
17. J. W. Mathews, in *Epitaxial Growth*, edited by J. W. Mathews (Academic, New York, 1975), Part B, Chap. 8.
18. J. W. Mathews, in *Dislocations in Solids*, edited by F. R. N. Nabarro (North-Holland, Amsterdam, 1979).
19. K.W. Schwarz, *Phys. Rev. Lett.* **91**, 145503 (2003).

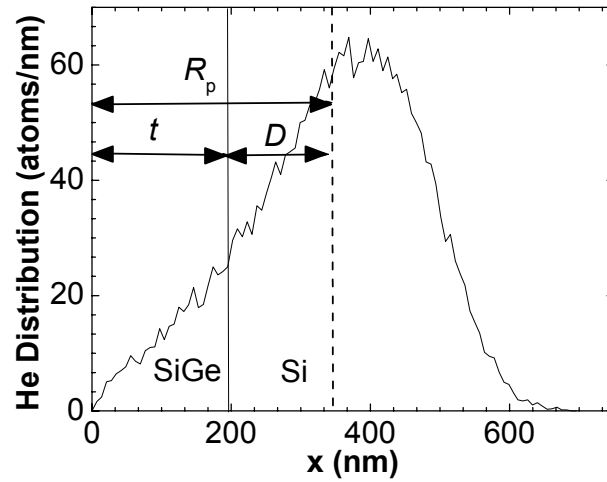


Fig. 1. A simulated helium profile of 38 keV He^+ implanted into a 196 nm $\text{Si}_{0.7}\text{Ge}_{0.3}/\text{Si}$ structure. R_p is the projected range of He, and t is SiGe layer thickness, and D is implantation depth with respect to the SiGe/Si interface. The total number of He atoms used in simulation is 20000.

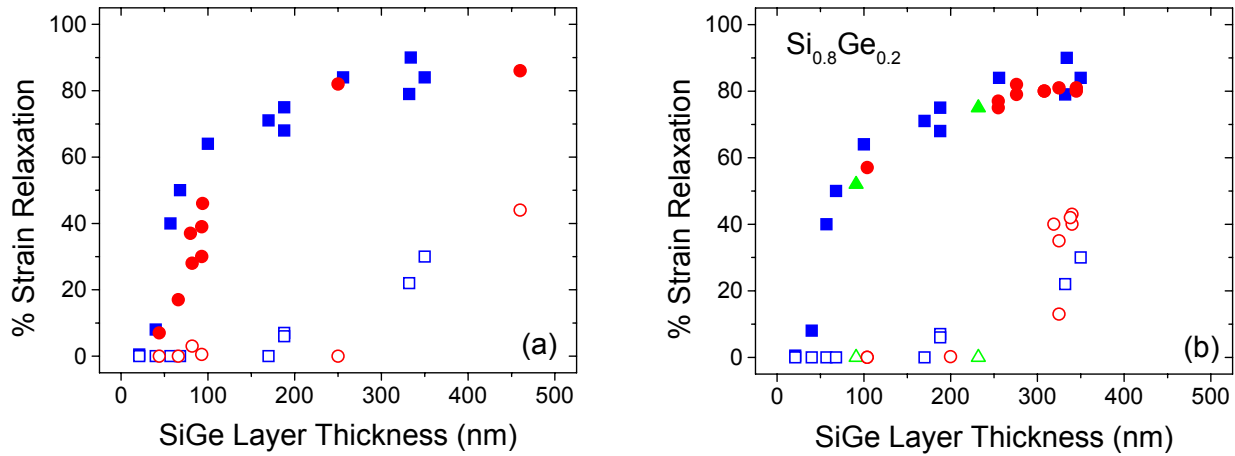


Fig. 2. (a) Strain relaxation of $\text{Si}_{1-x}\text{Ge}_x$ layers, $x=0.16$ (\bullet) and $x=0.20$ (\blacksquare), grown by UHVCVD on 200mm wafers. (b) Strain relaxation of $\text{Si}_{0.8}\text{Ge}_{0.2}$ layers grown in three different reactors: UHVCVD-200 (\blacksquare); RTCVD -200 (\bullet); and RTCVD-300 (\blacktriangle). Samples were annealed at 800 or 850 °C for at least 10 minutes. Open symbols are areas of the wafer that were not implanted. Solid symbols are areas that were implanted with $1 \times 10^{16} \text{ cm}^{-2}$ helium at a depth of 140-200 nm below the SiGe/Si interface. The error in the strain relaxation measured by XRD is $\sim \pm 3\%$.

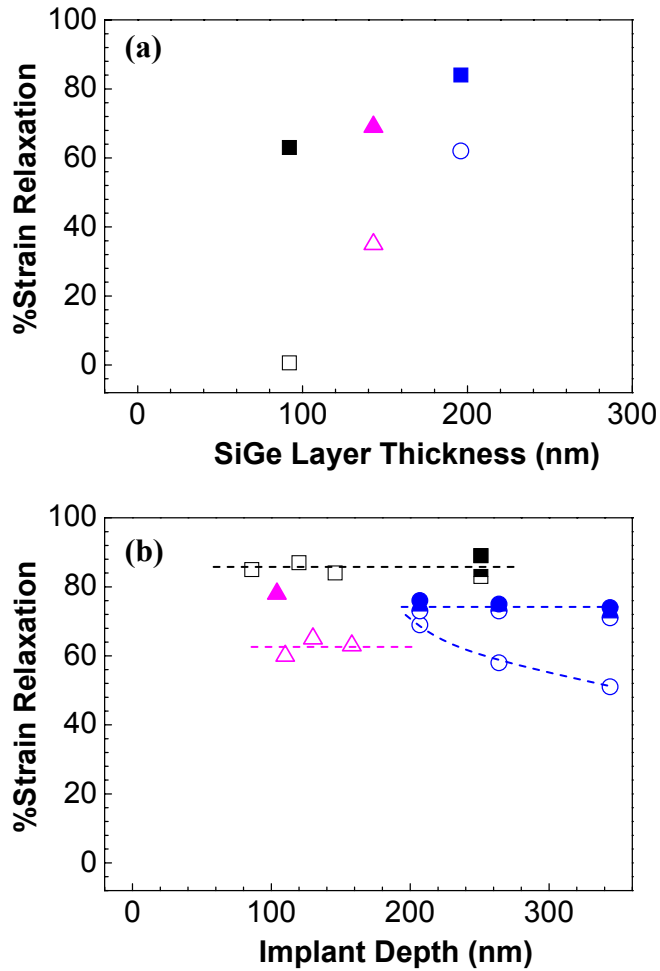


Fig. 3(a) Strain relaxation of $\text{Si}_{1-x}\text{Ge}_x$ layers grown by RTCVD, $x=0.3$. Open symbols are areas of the wafer that were not implanted. Solid symbols are areas that were implanted with 10^{16} cm^{-2} helium at a depth of 150-200 nm below the SiGe/Si interface. (b) Relaxation of $\text{Si}_{0.7}\text{Ge}_{0.3}$ layers with different thickness and implantation conditions. $\blacksquare, \bullet, \blacktriangle$ represent 196, 143 and 92 nm SiGe layers, respectively. Open, half filled and filled symbols represent helium implantation doses of 1, 1.5 and $2 \times 10^{16} \text{ cm}^{-2}$, respectively.

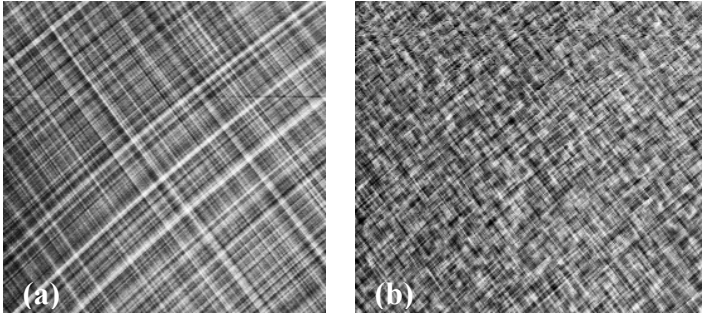


Fig. 4. AFM images of two types of surface features in implanted/annealed 196 nm $\text{Si}_{0.7}\text{Ge}_{0.3}$ layers: (a) regular cross-hatch patterns for deeper implanted samples ($D=146$ nm), and (b) patchy patterns for shallower implanted samples ($D=86$ nm). Helium dose is 10^{16} cm^{-2} in both cases. The shown images have an area of $15 \times 15 \mu\text{m}^2$.

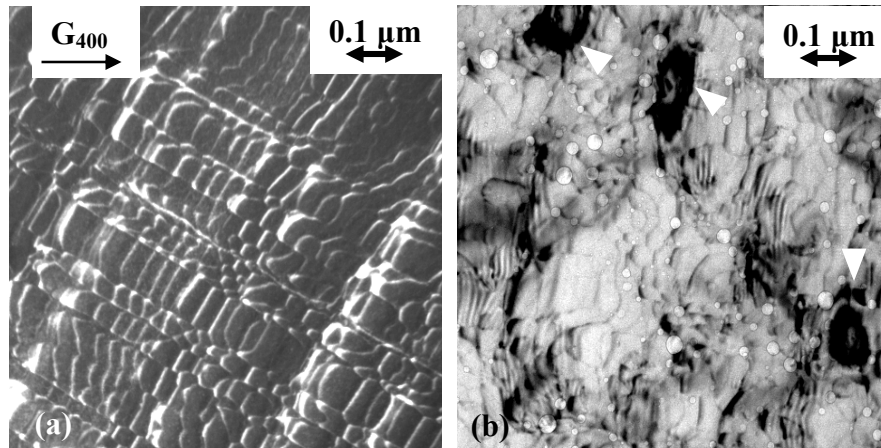


Fig. 5. Plan view TEM images of samples with low and high threading dislocations. (a) Dark field image shows the regular array of misfit dislocations in a 143 nm $\text{Si}_{0.7}\text{Ge}_{0.3}$ layer with threading dislocation density of $4.4 \times 10^7 \text{ cm}^{-2}$. The material is 74 % relaxed after annealing. (b) Bright field image taken at weak diffraction conditions shows both helium bubbles and the irregular misfit dislocation array in a 92 nm $\text{Si}_{0.7}\text{Ge}_{0.3}$ layer with threading dislocation density of $2.7 \times 10^{10} \text{ cm}^{-2}$. The material is 78% relaxed after annealing. Dark contrast areas indicated by arrows are regions of very high strain.

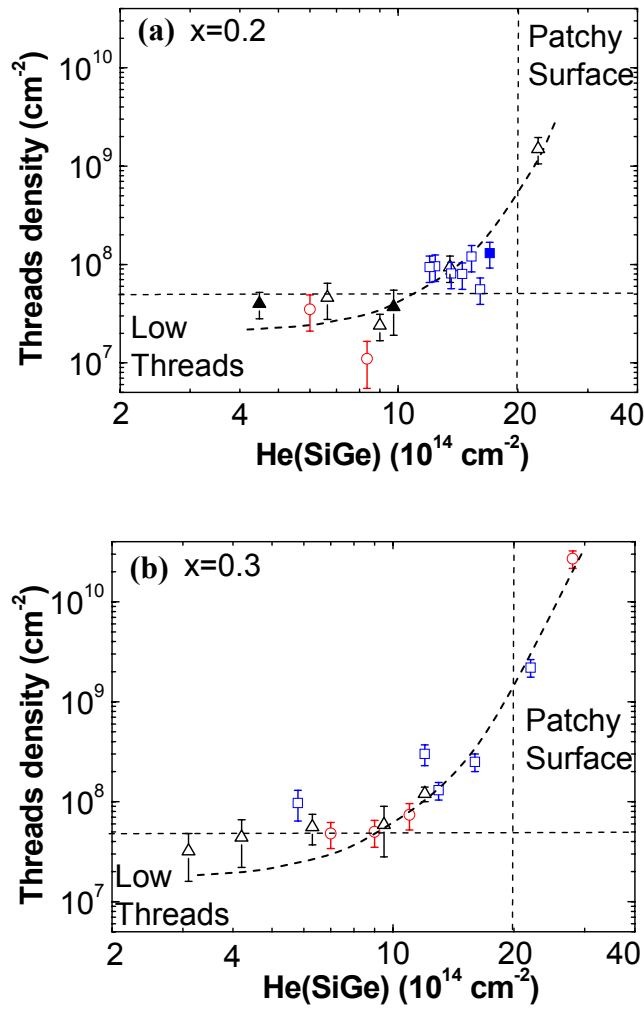


Fig. 6. Threading dislocation density increases with He(SiGe). Open and solid symbols are wafers grown by RTCVD and UHVCVD, respectively. Dashed lines are guides for the eye. (a) Threading dislocation density in Si_{0.8}Ge_{0.2} layers: ○ are 92 nm, 52% relaxed; ▲△ are 220 nm, 70% relaxed; ■□ are 320-340 nm, 80% relaxed. (b) Threading dislocation density in Si_{0.7}Ge_{0.3} layers: ○ are 92 nm, 60% relaxed; △ are 143 nm, 70% relaxed; □ are 196 nm, 85% relaxed.